

Reinforcement Slip in Reinforced Concrete Columns

by Halil Sezen and Eric J. Setzler

Reinforcement slip in footings and beam-column joint regions can make a significant contribution to the total lateral displacement of a reinforced concrete structure. In this paper, a model for the prediction of lateral deformation of a column due to reinforcement slip in the anchorage zone is presented. The model employs a stepped bond stress along the embedded length of the reinforcing bar that allows for efficient computation of displacements due to slip. A method for computing slip when a reinforcing bar is stressed to its unloaded end and a corresponding failure criterion are presented. Procedures for calculating slip in hooked bars are also outlined. The proposed model is compared with five other commonly-used models found in the literature against three independent sets of test data. Considering its simplicity and computational efficiency, the proposed model predicts slip displacements reasonably well.

Keywords: bond-slip; bond stress; columns; lateral loads; reinforced concrete.

INTRODUCTION

A reinforcing bar embedded in concrete subjected to tensile force will accumulate strain over the embedment length of the bar. This strain causes the reinforcing bar to extend, or slip, relative to the concrete in which it is embedded. The longitudinal reinforcement in a reinforced concrete column with fixed ends subjected to bending may be in tension at the beam-column or footing-column interface. Slip of the reinforcing bars outside the flexure length and in the anchoring concrete (that is, in the footing or beam-column joint region) will cause rigid-body rotation of the column as shown in Fig. 1. This rotation is additive to the rotation calculated from flexural analysis of the column. This increased rotation causes greater drift of columns, beams, and walls under lateral loads; therefore, it is important to account for reinforcement slip when determining the response of a reinforced concrete structure subjected to lateral loading. Experimental results from four double-curvature columns tested by Sezen¹ indicate that, in some cases, the deformations due to reinforcement slip may be as large as column flexural deformations. For these columns, slip deformations contributed 25 to 40% of the total lateral displacement.² This suggests that if deformations resulting from reinforcement slip are ignored in the member analysis, the predicted lateral deformations may be significantly underestimated or the predicted lateral stiffness may be overestimated.

In this paper, a stepped bond-stress model is proposed for the prediction of slip in reinforcing bars in tension. Procedures for dealing with slip at the unloaded end of straight bars and hooked bars are outlined. A relationship is given for calculating slip rotation, which is necessary for the prediction of the lateral displacement of columns due to slip. Data from the experimental investigations of columns from several previous studies are compared with the response predicted by the proposed model and five other commonly used slip models.

RESEARCH SIGNIFICANCE

Modeling the response of a reinforced concrete structure to lateral loading is complex. The total lateral deformation of a column is composed of three components, namely, flexural, bar slip, and shear deformations. For the accurate prediction of the overall structural behavior, each of these three deformation components must be considered. Modeling of an entire structure involves many members and is a time-consuming process, even with today's fast computers. Therefore, a computationally efficient model that can calculate reinforcement slip accurately is necessary for use as part of an overall structural response program. In this paper, a relatively simple bar slip deformation model is developed and evaluated using experimental data and other available models.

BACKGROUND AND PREVIOUS WORK

Numerous researchers have investigated the slip of reinforcing bars under tensile loading. The various models fall into two broad categories. Macro models deal with the average slip behavior and often assume a uniform or stepped bond stress over the development length of the reinforcing bar. Models by Otani and Sozen,³ Alsiwat and Saatcioglu,⁴ and Lehman and Moehle⁵ are of this kind. Macro models are very efficient from a computational standpoint. Micro models attempt to model the steel-concrete interface on a local level, and often use a varying bond stress-local slip relationship within a numerical model. Two notable studies that have investigated the local bond phenomena closely are by Eligehausen et al.⁶ and Hawkins et al.⁷ Micro models tend to agree well with experimental data, but they require several nested iteration loops over the embedment length of the bar

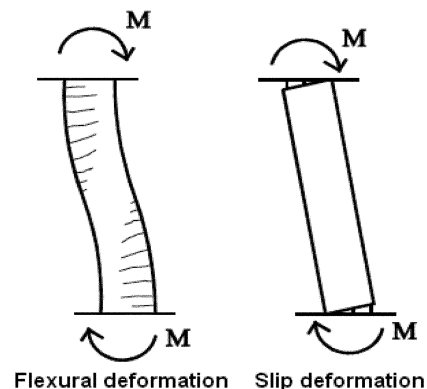


Fig. 1—Flexural and slip deformations in reinforced concrete column.

ACI Structural Journal, V. 105, No. 3, May-June 2008.

MS No. S-2006-180.R1 received January 20, 2007, and reviewed under Institute publication policies. Copyright © 2008, American Concrete Institute. All rights reserved, including the making of copies unless permission is obtained from the copyright proprietors. Pertinent discussion including author's closure, if any, will be published in the March-April 2009 *ACI Structural Journal* if the discussion is received by November 1, 2008.

ACI member **Halil Sezen** is an Assistant Professor of civil engineering at Ohio State University, Columbus, OH. He received his BSCE from the Middle East Technical University, Ankara, Turkey; his MS from Cornell University, Ithaca, NY; and his PhD from the University of California-Berkeley, Berkeley, CA. He is a member of ACI Committees 341, Earthquake Resistant Concrete Bridges; 369, Seismic Repair and Rehabilitation; 562, Evaluation, Repair, and Rehabilitation of Concrete Buildings; and Joint ACI-ASCE Committee 445, Shear and Torsion. His research interests include the design and behavior of concrete structures and earthquake engineering.

Eric J. Setzler is a Structural Engineer with Burgess & Niple, Inc., Painesville, OH. He is a former Graduate Fellow in the Department of Civil and Environmental Engineering and Geodetic Science at Ohio State University, where he received his BS and MS. His research interests include the design and behavior of concrete structures.

to achieve equilibrium. This makes the application of these models computationally intense. The model by Eligehausen et al.⁶ has seen wide use in slip modeling, and many researchers⁸⁻¹⁰ have proposed additions or modifications to their model.

A reinforcing bar embedded in concrete can be modeled by assuming linear elastic behavior and a uniform bond stress u_b over the development length l_d of the reinforcing bar, as shown in Fig. 2(a). From equilibrium of forces, the force in the bar F is

$$F = f_s A_b = u_b \pi d_b l_d \quad (1)$$

where f_s is the steel stress, A_b is the steel area, and d_b is the bar diameter. By substituting for the area of the bar, the required development length can be determined

$$l_d = \frac{f_s d_b}{4u_b} \quad (2)$$

The stress in the bar decreases linearly from f_s at the loaded end to zero at the development length. Therefore, the slip of the bar (slip) can be determined from integrating the strains over the development length

$$\text{slip} = \frac{\varepsilon_s l_d}{2} = \frac{f_s l_d}{2E_s} = \frac{f_s^2 d_b}{8E_s u_b} \quad (3)$$

where E_s is the steel modulus of elasticity. Note that Eq. (3) assumes that the embedment length of the bar is longer than the development length calculated from Eq. (2). In one of the earliest studies on slip, Otani and Sozen³ assumed an average uniform bond stress of $u_b = 0.54 \sqrt{f'_c}$ MPa ($6.5 \sqrt{f'_c}$ psi) for embedded bars in tension, where f'_c is the concrete compressive strength in MPa (psi).

Based on experiments, Lehman and Moehle⁵ and Saatcioglu et al.¹¹ demonstrated that at the beam-column interface, strains in the reinforcing bar can be much larger than the yield strain, causing columns to experience significant fixed-end rotations. Based on tests of bridge columns, Lehman and Moehle⁵ proposed a stepped bond stress-slip model. In this model, for slip values less than the slip corresponding to the yield strain in the bar, the uniform bond stress is taken as $u_b = 1.0 \sqrt{f'_c}$ MPa ($12 \sqrt{f'_c}$ psi). For slip values exceeding the slip at yield, the bond stress capacity is $u_b = 0.5 \sqrt{f'_c}$ MPa ($6 \sqrt{f'_c}$ psi).

An analytical procedure was proposed by Alsiwat and Saatcioglu⁴ to predict the monotonic force-deformation relationship of a reinforcing bar embedded in concrete using a stepped bond stress distribution (Fig. 2(b)). According to

this model, four regions are developed along a reinforcing bar in tension, namely, an elastic region with length L_e , a yield plateau region with length L_{yp} , a strain-hardening region with length L_{sh} , and a pullout-cone region with length L_{pc} . An elastic uniform bond stress u_e is assumed along the elastic length, whereas a frictional uniform bond stress u_f is assumed in the yield plateau and strain-hardening regions. The elastic bond stress was adopted from ACI Committee 408¹² and is equal to $0.87 \sqrt{f'_c}$ MPa ($10.5 \sqrt{f'_c}$ psi) for most applications. The frictional bond stress is based on the results of an experimental investigation by Pochanart and Harmon.¹³ The slip is calculated by integrating the strains over the development length, and it is the area under the strain diagram shown in Fig. 2(b).

The model by Hawkins et al.⁷ uses a trilinear curve to relate the bond stress to the local slip at each location along the embedded length of the bar. Eligehausen et al.⁶ use a similar curve. Each of these two models was derived from tests of pullout specimens conducted by the respective authors. The bond stress-slip displacement relations, as defined in these models, are shown in Fig. 3, and the effects of parameters that define them are discussed in the literature.^{6,7,14}

PROPOSED REINFORCEMENT SLIP MODEL

A macro-level approach was used for the proposed slip model, and it was assumed that the bond stress could be approximated as a stepped function, with a value u_b for elastic steel stresses, and u_b' for stresses greater than the yield stress. Because the model is intended to be used in the analysis of entire structures, a macro-model approach is appropriate. This approach allows efficient computation of slip by eliminating the need for nested iteration loops that are required in numerical models. Based on this selection, the slip can be determined by integrating the strain over the development length as follows

$$\text{slip} = \int_0^{l_d + l'_d} \varepsilon(x) dx \quad (4)$$

where l_d and l'_d are the development lengths for the elastic and inelastic portions of the bar, respectively. Because the

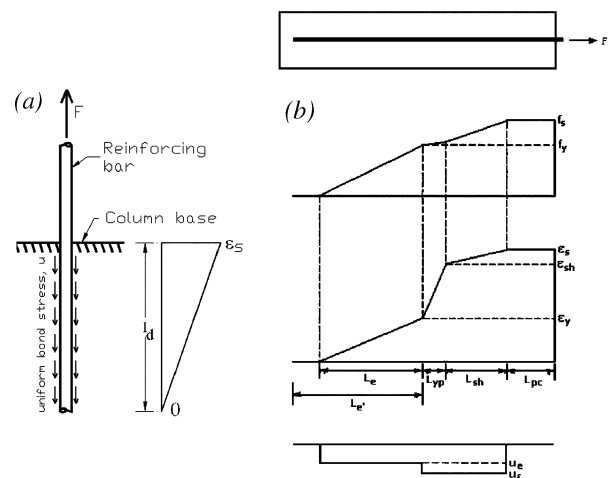


Fig. 2—(a) Elastic bond stress model; and (b) bond stress model by Alsiwat and Saatcioglu.⁴

bond stress is uniform in each range, the strain distribution will be bilinear, as shown in Fig. 4. Carrying out the integration of Eq. (4) yields

$$\text{slip} = \frac{\epsilon_s l_d}{2} \quad \text{for } \epsilon_s \leq \epsilon_y \quad (5)$$

$$\text{slip} = \frac{\epsilon_y l_d}{2} + \frac{(\epsilon_s + \epsilon_y) l_d'}{2} \quad \text{for } \epsilon_s > \epsilon_y$$

The development lengths can be determined from equilibrium of forces along the bar. Equation (2) applies to the elastic range (with f_s limited by f_y), and the following equation can be derived for the inelastic range

$$l_d' = \frac{(f_s - f_y) d_b}{4 u_b'} \quad (6)$$

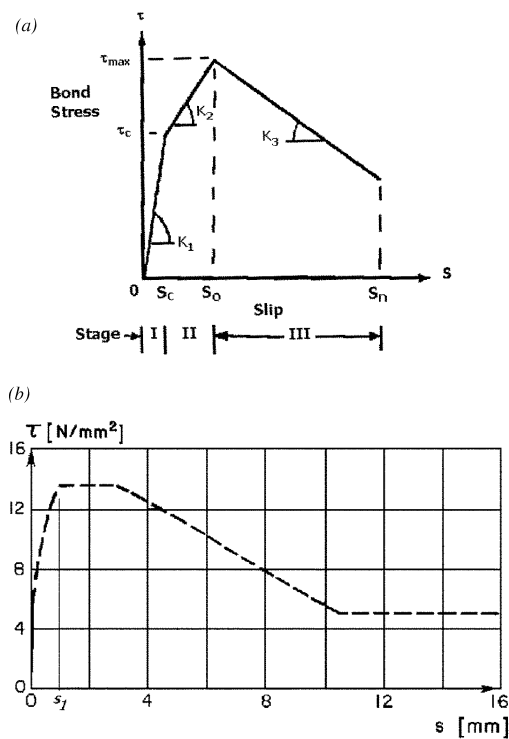


Fig. 3—Bond stress models by: (a) Hawkins et al.⁷; and (b) Eligehausen et al.⁶

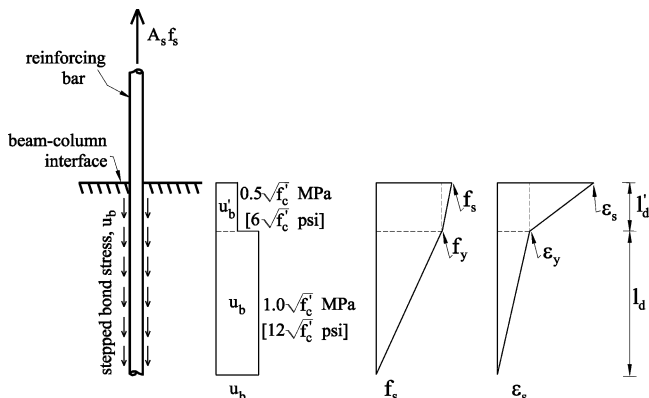


Fig. 4—Proposed reinforcement slip model.

Uniform bond stresses

The slip was measured at the ends of 12 column specimens tested by Sezen¹ and Lynn et al.¹⁵ Using the measured slip values at yield displacement, uniform bond stresses u_{by} were calculated. The calculated bond stresses are divided by the square root of the concrete strength and presented in Fig. 5. For the 12 columns considered, the average bond stress is $0.95 \sqrt{f_c'}$ MPa ($11.4 \sqrt{f_c'}$ psi), and the standard deviation is $0.21 \sqrt{f_c'}$ MPa ($2.5 \sqrt{f_c'}$ psi). Sozen and Moehle¹⁶ calculated a mean average bond strength of $0.83 \sqrt{f_c'}$ MPa ($10.0 \sqrt{f_c'}$ psi) from 35 beam tests under monotonic loading. All beams had a clear cover-to-bar-diameter ratio smaller than or equal to 2.5 ($c/d_b \leq 2.5$) with single or multiple No. 8 (25 mm) longitudinal bars with or without stirrups. Melek et al.¹⁷ also obtained an average bond strength of $u_b = 0.95 \sqrt{f_c'}$ MPa ($11.4 \sqrt{f_c'}$ psi) based on strains measured on 15 longitudinal bars in six test columns with lap splices. Based on this test data, in this study, a uniform bond stress of $u_b = 1.0 \sqrt{f_c'}$ MPa ($12 \sqrt{f_c'}$ psi) is assumed in the elastic range (Fig. 4). In the portion of the reinforcing bar over which the yield strain is exceeded, a uniform bond stress of $u_b' = 0.5 \sqrt{f_c'}$ MPa ($6 \sqrt{f_c'}$ psi) is adopted from the study by Lehman and Moehle.⁵ Figure 6 shows two examples of measured cyclic bond stresses and the bond-slip model.

Slip rotation

Once the slip of a reinforcing bar is known, the rotation of the column caused by this slip must be determined. For the proposed model, it is assumed that slip will occur in bars under tension only, and that the rotation will be about the neutral axis. As illustrated in Fig. 7, the slip rotation θ_s can be calculated by dividing the bar slip by the depth of the open crack, which is the difference between the depth of the section d and the neutral axis depth c .

$$\theta_s = \frac{\text{slip}}{d - c} \quad (7)$$

By combining Eq. (2), (5), (6), and (7), a compact set of equations can be derived for the calculation of slip rotation

$$\theta_s = \frac{\epsilon_s f_s d_b}{8 u_b (d - c)} \quad \text{for } \epsilon_s \leq \epsilon_y \quad (8)$$

$$\theta_s = \frac{d_b}{8 u_b (d - c)} (\epsilon_y f_y + 2(\epsilon_s + \epsilon_y)(f_s - f_y)) \quad \text{for } \epsilon_s > \epsilon_y$$

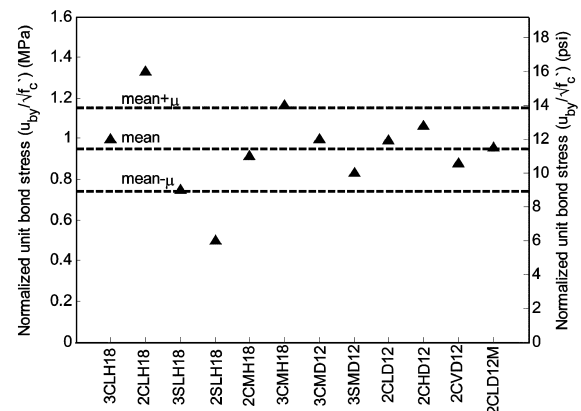


Fig. 5—Calculated bond stresses at yield level.

Slip at unloaded end of bar

The development length calculated using the proposed model ($l_d + l'_d$), as shown in Fig. 4) will often be greater than the provided embedment length. The Eligehausen model⁶ shows that when a bar is stressed up to its unloaded end (that is, when the embedment length is less than the calculated development length), the end of the bar slips to mobilize bond strength and satisfy equilibrium. A uniform or stepped bond stress model, however, cannot directly account for slip at the unloaded end because increasing slip does not increase the bond capacity of the bar. Therefore, an alternate approach must be employed.

It can be shown from the Eligehausen model that a bar with an embedment length l_{embed} shorter than the embedment length required to cause bar fracture before pullout, l_{fr} , will behave similarly to a bar with an embedment length greater than l_{fr} up to the point of pullout. The behavior of a No. 10 bar embedded in 27.6 MPa (4000 psi) concrete is calculated using the Eligehausen model as the embedment length is varied from 200 to 500 mm (7.9 to 19.7 in.), and the results are shown in Fig. 8. For any embedment length longer than l_{fr} (approximately 400 mm [15.7 in.]¹⁸), the behavior is essentially identical, and the tensile strength of the bar is exceeded before the bar pulls out of the concrete. As the embedment length is decreased, the bar pulls out at progressively lower stresses, but the ascending portion of the curve is still similar to the curve for a long bar. If the bar pulls out before reaching a stress of approximately f_y at the loaded end (that is, $l_{embed} <$ approximately 300 mm [11.8 in.] in Fig. 8), however, the behavior is not as similar to the

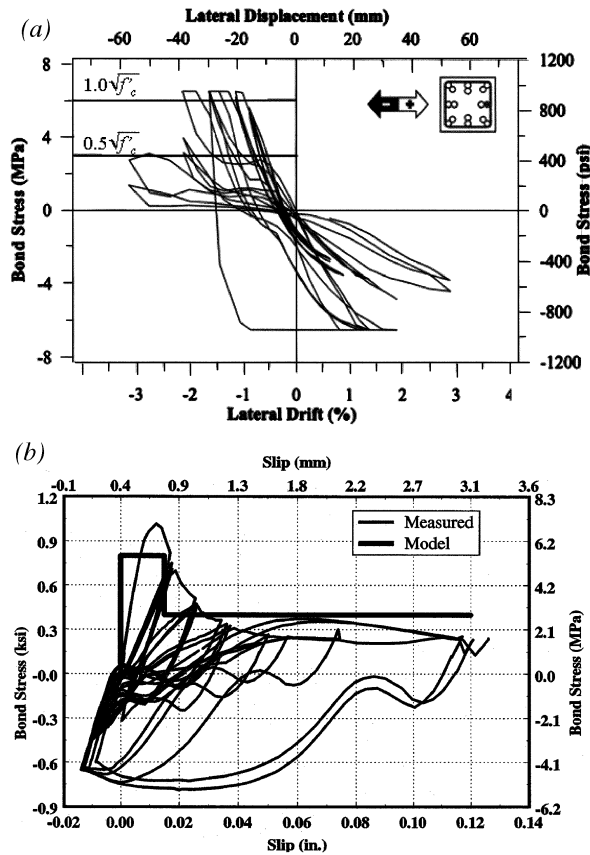


Fig. 6—(a) Bond stress measured in longitudinal column bar¹⁵; and (b) bond stress-slip data and model by Lehman and Moehle.⁵

long-bar behavior. For example, for an embedment length of 310 mm (12.2 in.) in Fig. 8, the response closely follows the response of the bars with embedment lengths greater than 400 mm (15.7 in.) all the way to its peak strength. The bar with an embedment length of 270 mm (10.6 in.), however, starts to noticeably deviate from the long-bar curve around a force of 150 kN (33.7 kip), although its peak strength is almost 200 kN (45.0 kip). These observations suggest that the proposed model can be applied to bars with embedment lengths less than l_{fr} , but greater than some minimum length, if the point of pullout can be predicted.

A parametric study was conducted to determine a relationship for the minimum embedment length, $l_{d,min}$, necessary for the force-bar slip response of a reinforcing bar to be similar to that of a bar with a very long embedment length.¹⁸ Sixty pullout specimens with different material properties and dimensions were modeled using the Eligehausen bond-slip model (Fig. 3(b)). For each specimen, the embedment length was varied as shown in Fig. 8, and $l_{d,min}$ was noted. By comparing these minimum lengths with the parameters that were varied in each specimen, it was determined that the main variables affecting the minimum required embedment length were the bar diameter d_b , the steel yield stress f_y , and the concrete compressive strength f'_c . The best relationship between the minimum embedment length and the variables

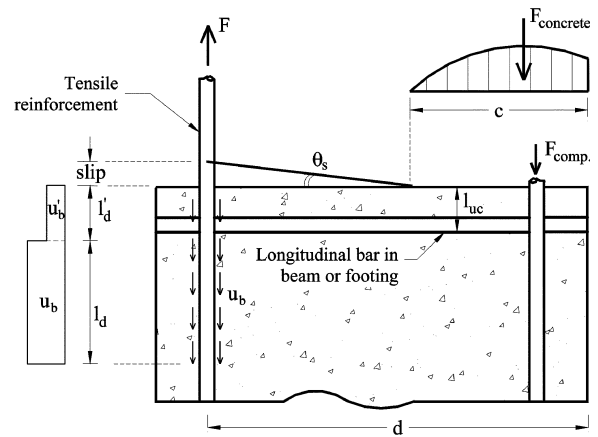


Fig. 7—Calculation of slip rotation in proposed model.

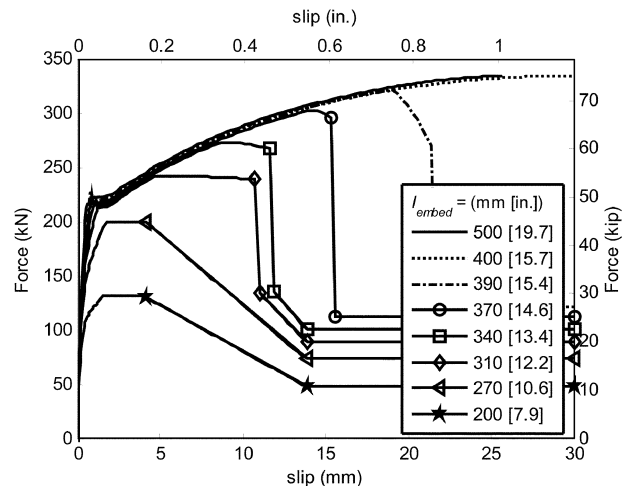


Fig. 8—Slip behavior of bar as function of embedment length.

noted previously was achieved by plotting $l_{d,min}$ versus the product $d_b f_y / \sqrt{f'_c}$, as shown in Fig. 9. From a linear regression analysis of the calculated data, it was determined that the minimum embedment length necessary to treat the bar as if it were very long can be best modeled as

$$l_{d,min} - l_{uc} = 0.088 \frac{d_b f_y}{\sqrt{f'_c}} + 35.6 \quad (9)$$

$$\left[l_{d,min} - l_{uc} = 0.0073 \frac{d_b f_y}{\sqrt{f'_c}} + 140 \right]$$

where l_{uc} is the depth of unconfined cover concrete in the joint or footing, as shown in Fig. 7. For all equations in this section, lengths are in mm (in.) and stresses are in MPa (psi). The depth of the cover concrete is subtracted from $l_{d,min}$ in Eq. (9) because it was ineffective in providing the required embedment length in the study.

The ACI 318-05¹⁹ equation for development length is

$$l_{d,ACI} = \left(0.9 \frac{f_y}{\sqrt{f'_c}} \frac{\psi_t \psi_e \psi_s \lambda}{\left(\frac{c_b + K_{tr}}{d_b} \right)} \right) d_b \quad (10)$$

$$\left[l_{d,ACI} = \frac{f_y}{\sqrt{f'_c}} \frac{\psi_t \psi_e \psi_s \lambda}{\left(\frac{c_b + K_{tr}}{d_b} \right)} d_b \right]$$

where ψ_t is the reinforcement location factor (1.3 for top bars, 1.0 otherwise); ψ_e is the epoxy coating factor (1.0 for uncoated bars) with $\psi_t \psi_e \leq 1.7$; ψ_s is the reinforcement size factor (0.8 for No. 6 or smaller size bars, and 1.0 for larger bars); $\lambda = 1.0$ for normalweight concrete and 1.3 for lightweight concrete; c_b is the smaller of the distance from the center of a bar to the nearest concrete surface, and one-half the center-to-center spacing of bars being developed; and K_{tr} is the transverse reinforcement index.¹⁹ Many common construction situations result in a value $(c_b + K_{tr})/d_b$ of at least 1.5.¹⁹ Assuming that the factors ψ_t , ψ_e , ψ_s , and λ are 1.0 for most applications, Eq. (10) simplifies to

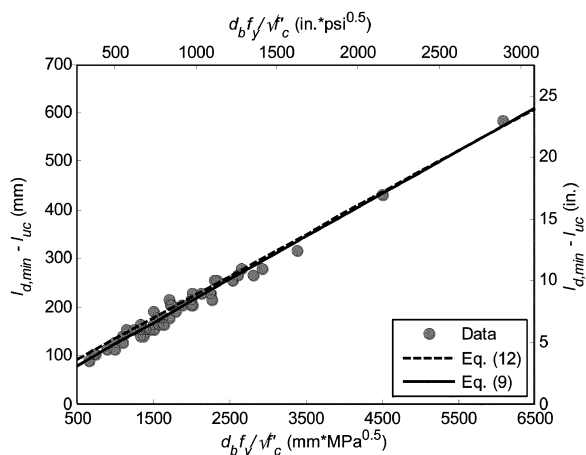


Fig. 9—Minimum embedment length $l_{d,min}$.

$$l_{d,ACI} = 0.6 \frac{d_b f_y}{\sqrt{f'_c}} \left[l_{d,ACI} = 0.05 \frac{d_b f_y}{\sqrt{f'_c}} \right] \quad (11)$$

By substituting this relationship into Eq. (9) and rounding, Eq. (9) can be approximated as

$$l_{d,min} - l_{uc} = \frac{l_{d,ACI}}{7} + 50 \left[l_{d,min} - l_{uc} = \frac{l_{d,ACI}}{7} + 2 \right] \quad (12)$$

For common situations, the distance l_{uc} will be approximately 75 mm (3 in.). This assumes 38 mm (1.5 in.) for concrete cover, 12 mm (0.5 in.) for the transverse bar, and 25 mm (1 in.) for the longitudinal bar. Therefore, the minimum embedment length can be calculated as

$$l_{d,min} = \frac{l_{d,ACI}}{7} + 125 \left[l_{d,min} = \frac{l_{d,ACI}}{7} + 5 \right] \quad (13)$$

Equation (12) is compared with the data in Fig. 8. Note that Eq. (13) does not suggest a revision of the ACI development length, which is intended to achieve a long-bar slip behavior with bar fracture occurring at the loaded end after yielding (that is, $l_{d,ACI} > l_{fr} = 400$ mm [15.7 in.] in Fig. 8). Rather, Eq. (13) gives an estimate for the minimum embedment length necessary for the application of the proposed slip model. This minimum length is the length where the bar will pull out just as it reaches the yield strength f_y at the loaded end (that is, $l_{d,min} =$ approximately 300 mm [11.8 in.] in Fig. 8). Thus, the embedment lengths calculated from Eq. (13) are typically smaller than those found in actual construction.

The local slip will increase over the length of a bar from a minimum at the unloaded end up to a maximum at the loaded end. The Eligehausen bond-slip model (Fig. 3(b)) predicts that when the slip at the unloaded end of the bar reaches a value of s_1 , there is no way for more capacity to be developed and the bar will pull out of the anchoring concrete with any increase in force. Therefore, this value can be used as a criterion for the onset of pullout failure. Eligehausen⁶ states that s_1 can be taken as 1.0 mm (0.039 in.) for concrete strengths of 30 MPa (4350 psi), and for other concrete strengths, this value can be reduced approximately proportionally to the square root of f'_c . This criterion is selected for the proposed model. Eligehausen also recommends modifying the value of s_1 based on the bar lug geometry (related rib area). Further studies,⁹ however, have shown that s_1 is largely independent of lug geometry for a common range of values.

As discussed previously, the slip behavior of a bar in which stress penetrates to the unloaded end (that is, $l_{embed} < l_d + l'_d$) is very similar to the slip behavior of an identical bar with very long embedment length, up to the point of pullout. Therefore, the slip at the unloaded end of the former bar can be calculated using the strain diagram of the latter bar (Fig. 4). First, the strain at the unloaded end of the actual bar, ϵ_{end} is calculated using similar triangles (Eq. (14a) was derived assuming the end of the actual bar is within the elastic bond stress region). Then, the slip at the unloaded end of the actual bar is calculated as the area under the strain diagram past the unloaded end of the bar.

$$\varepsilon_{end} = \left(1 - \frac{l_{embed} - l'_d}{l_d}\right) \varepsilon_e \quad (14a)$$

$$s_{end} = \frac{1}{2} \varepsilon_{end} [(l_d + l'_d) - l_{embed}] \quad (14b)$$

where ε_e is the maximum strain in the elastic portion of the bar. The bar will fail by pulling out of the anchoring concrete when the slip at the unloaded end of the bar, s_{end} , exceeds s_1 , given by

$$s_1 = 1.0 \sqrt{\frac{30}{f'_c}} \left[s_1 = 0.039 \sqrt{\frac{4350}{f'_c}} \right] \quad (15)$$

In summary, for straight bars with an embedded length not less than $l_{d,min}$, computed by Eq. (13), the slip may be calculated using the stepped bond stress model presented herein, which assumes that the embedment length is greater than the development length calculated from Eq. (2) and (6). It is assumed that a pullout failure will initiate if the slip at the unloaded end of the bar exceeds s_1 , calculated from Eq. (15).

Hooked bars

It is common practice to use hooks for anchorage of reinforcing bars in exterior beam-column joints and in column-footing connections. Hooks change the mechanics of the bond phenomena because the applied force is resisted by both the bond over the straight length and a bearing mechanism over the bent length. Depending on the applied stress, strain may penetrate into the hook. Several methods for modeling the slip of a hooked bar were investigated.¹⁸ Based on experimental data, Filippou et al.⁸ suggested that a hooked bar can be modeled as a straight bar with an equivalent length of

$$l_{eq} = l_s + 5d_b \quad (16)$$

where l_s is the straight embedment length. This recommendation is adopted for the proposed model.

COMPARISON OF MODELS AND EXPERIMENTAL DATA

Bar slip comparisons

The purpose of this study is to develop a simple and computationally efficient model that can predict the section rotation caused by reinforcement slip with reasonable accuracy. First, the capability of the model to predict the slip of a single bar embedded in concrete is investigated. Test results for 22 pullout specimens, each of which consists of a single straight or hooked bar embedded in a block of concrete, are reported in Ueda et al.¹⁴ Six specimens, named S101, S107, B103, B81, S61, and S64, are used herein for comparison of the various models. Specimens S101 and S107 are No. 10 straight bars and Specimens S61 and S64 are No. 6 straight bars. Specimens B103 and B81 are a No. 10 and a No. 8 hooked bar, respectively. Properties of these specimens are summarized in Table 1. Steel constitutive relationships for the test specimens were given in the work by Ueda et al.¹⁴ These were modeled using a linear relationship up to the yield stress, a plateau with zero slope up to the onset of strain hardening at a strain of ε_{sh} , and a quadratic function for the strain hardening region, given as

$$f_s = f_u - (f_u - f_y) \left(\frac{\varepsilon_{su} - \varepsilon_s}{\varepsilon_{su} - \varepsilon_{sh}} \right)^2 \quad (17)$$

where f_u and ε_{su} are the ultimate stress and strain. Stress and strain values used in the model are given in Table 1.

Models by Otani and Sozen,³ Alsiwat and Saatcioglu,⁴ Eligehausen et al.,⁶ and Hawkins et al.⁷ and the proposed model are used to predict the slip response of the six test specimens. Test results for the specimens and predicted responses from the models are compared in Fig. 10. As described previously, the Otani-Sozen model³ assumes a uniform elastic bond stress, as well as linear elastic behavior of the reinforcing steel. Therefore, this model fails to capture the inelastic response as the yield stress of the bar is exceeded. The Alsiwat-Saatcioglu⁴ and proposed models initially tend to predict stiffer responses than the Eligehausen⁶ and Hawkins⁷ models. This trend reverses at higher stresses, however, and the Alsiwat-Saatcioglu⁴ and proposed models tend to predict lower forces for a given slip in the inelastic range. Ueda et al.¹⁴ notes that Specimens S107, B103, and S61 were loaded cyclically, so the last data point represents the point where the loading was reversed, and not the point of failure. Also, the connection between the loading equipment and bar failed on Specimen S64, which caused loading to cease prematurely. This explains why the test data for these four specimens end before the predictions of every model (all of which assume monotonic loading to failure). The force-slip response predictions of the Alsiwat-Saatcioglu⁴ and proposed models are similar for all tests. For Specimens S101 and B81, however, where the test data goes all the way to failure, the proposed model predicts the slip at failure better than the Alsiwat-Saatcioglu⁴ model. The average error of the predicted slip at failure is 25% for the proposed model and 79% for the Alsiwat-Saatcioglu⁴ model.

Overall, the proposed model compares very well with the other models in this study. For the specimens examined, the proposed model predicts forces less than or equal to the experimental force necessary to cause a given slip. In the analysis of a structure, this would lead to conservative estimates of overall strength and stiffness. While the proposed model tends to be less accurate than the Eligehausen⁶ and Hawkins⁷ models, it is still acceptably close. The maximum difference at any point between the proposed model and any of the other models is approximately 15 to 20%, and in most instances, the difference is much less than

Table 1—Properties of pullout specimens tested by Ueda et al.¹⁴

Name	Bar size	d_b , mm (in.)	l_{embed}^* , mm (in.)	f'_c , MPa (ksi)	f_y , MPa (ksi)	f_u , MPa (ksi)	ε_{sh}	ε_{su}
S101	No. 10	32.3 (1.27)	610 (24.0)	19.9 (2.89)	414 (60.1)	661 (95.9)	0.0101	0.0753
S107	No. 10	32.3 (1.27)	610 (24.0)	18.2 (2.64)	332 (48.1)	548 (79.5)	0.0163	0.0958
B103	No. 10	32.3 (1.27)	375 (14.75)	20.6 (2.98)	414 (60.1)	661 (95.9)	0.0101	0.0753
B81	No. 8	25.4 (1.00)	457 (18.0)	22.6 (3.28)	469 (68.0)	845 (122.5)	0.0037	0.1072
S61	No. 6	19.1 (0.75)	406 (16.0)	23.8 (3.45)	439 (63.6)	776 (112.5)	0.0041	0.0955
S64	No. 6	19.1 (0.75)	610 (24.0)	28.8 (4.17)	439 (63.6)	776 (112.5)	0.0041	0.0955

*For hooked bars, straight embedment length l_s is given.

that. This is an acceptable margin, considering that the experimental scatter in bond strengths can vary by a similar amount for nominally identical tests.⁶ Therefore, it appears that the proposed model can be used to predict the slip of a straight or hooked reinforcing bar embedded in concrete. Its simplicity should allow efficient calculation of the predicted slip behavior.

Rotation due to bar slip

If the force-slip relationship for a bar embedded in concrete is known, the rotation of a concrete section due to slip may be calculated using the moment-curvature relationship for the section and an assumption about the point about which slip rotation occurs. The various models compared in this study use different methods of calculating slip rotation. The Otani-Sozen³ model uses the following definition

$$\theta_s = \frac{\text{slip}}{d - d'} \quad (18)$$

where $(d - d')$ is the distance between the tensile and compressive reinforcing steel bars. Lehman and Moehle⁵ define the rotation of a section due to slip as

$$\theta_s = \frac{\text{slip}_t - \text{slip}_c}{d - d'} \quad (19)$$

where slip_t and slip_c are the signed values of bar slip in the tension and compression steel, respectively. Equation (7) is used for slip rotation computation in the other four models. The effect of axial load, which is pertinent in the behavior of a column, is accounted for in the moment-curvature analysis. Furthermore, in the proposed model and other models that calculate slip rotation using Eq. (7), axial load affects the calculated rotation through its effect on the neutral axis

depth. The models are compared in this section against two sets of column tests. Dimensions and material properties for the test columns are summarized in Table 2.

Saatcioglu et al.¹¹ tested five reinforced concrete cantilever columns and investigated bar slip behavior. Three of these are compared in this study: Columns B2, U4, and U6. Columns U4 and U6 were loaded cyclically in one direction, while Column B2 was loaded cyclically in the two perpendicular directions, although forces applied in one direction were kept below the force corresponding to the yield point. The authors of that study¹¹ found that displacements less than the yield displacement in one direction do not significantly affect behavior in the perpendicular direction. A typical cross section of the columns is shown in Fig. 11(a). The models are compared with test data for Saatcioglu's columns in Fig. 12. The Otani-Sozen³ model is shown for Column B2 only. It does a reasonable job of predicting the slip response before yielding; however, it does not capture the inelastic response of the column. This model shows similar trends for all seven columns, and will not be discussed further. The Eligehausen,⁶ Hawkins,⁷ Alsiwat-Saatcioglu,⁴ Lehman-Moehle,⁵ and proposed models all yield rather similar moment-slip rotation relationships. In the post-yield range, all models overestimate the moment necessary to cause a given rotation for Column B2. This could be due to differences between the material models used in this study and the actual properties. Overall, the predictions of the proposed model are acceptably close. In the inelastic range, the proposed model predictions are closer to the experimental data than the more detailed numerical models by Eligehausen⁶ and Hawkins.⁷

Four full-scale columns bent in double-curvature were tested by Sezen.¹ A typical section is shown in Fig. 11(b). All columns were subjected to unidirectional cyclic loading. The various models are compared with the experimental data for these columns in Fig. 13, which shows plots for

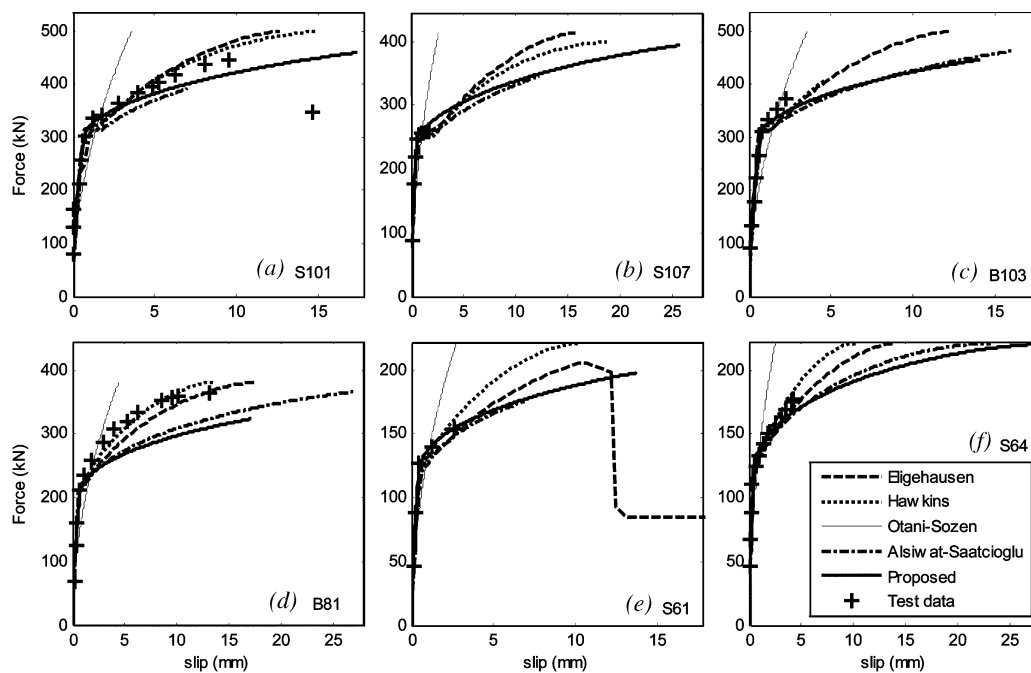


Fig. 10—Slip predictions for pullout tests: (a) Specimen S101; (b) Specimen S107; (c) Specimen B103; (d) Specimen B81; (e) Specimen S61; and (f) Specimen S64. (Note: 25.4 mm = 1 in.; 1 kN = 0.225 kip.)

moment-slip rotation at the base of each column. Only the Eligehausen,⁶ Alsiwat-Saatcioglu,⁴ and proposed models are shown in Fig. 13 due to space limitations. It is not obvious which model does the best job of predicting the overall slip behavior of the columns. In the early stages, the Alsiwat-Saatcioglu⁴ and proposed models tended to overestimate the response stiffness. This can be at least partially attributed to their assumption that the slip is zero for bars in compression. The Eligehausen⁶ model is closer to the observed behavior in this range. As the stresses increase, however, all models predict similar behavior.

One difficulty encountered in the proposed model is that Eq. (6) yields an inelastic development length l'_d of zero if

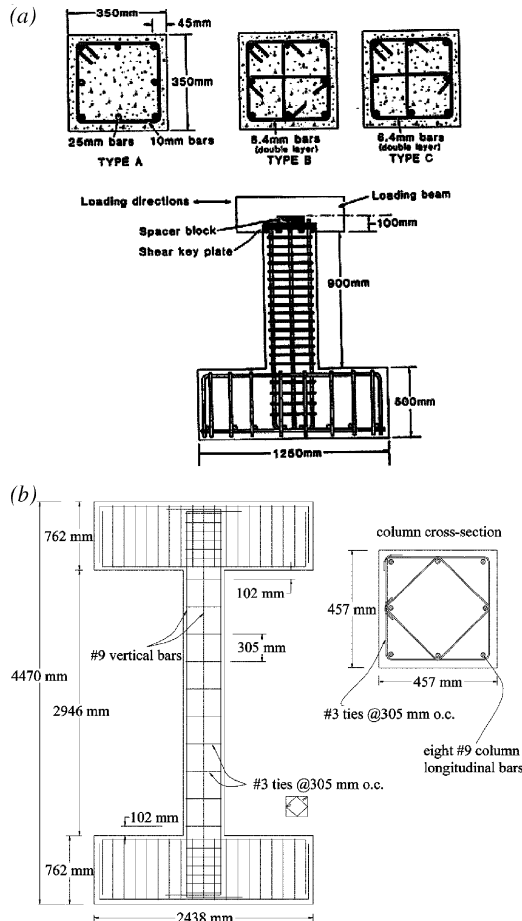


Fig. 11—Specimens tested by: (a) Saatcioglu et al.¹¹; and (b) Sezen.¹

the steel strain is within the yield plateau region and the yield plateau has zero slope. This means that as the bar extends from the yield strain to the start of strain hardening, no additional slip is recorded. This prediction does not agree with the expected behavior. To avoid this problem, using a modest strain hardening on the yield plateau is recommended. In this study, a slope of $E_{yp} = 2\%$ of E_s is used for modeling the test columns. This problem also occurs in the Alsiwat-Saatcioglu⁴ model, and is noted by those authors in the literature.

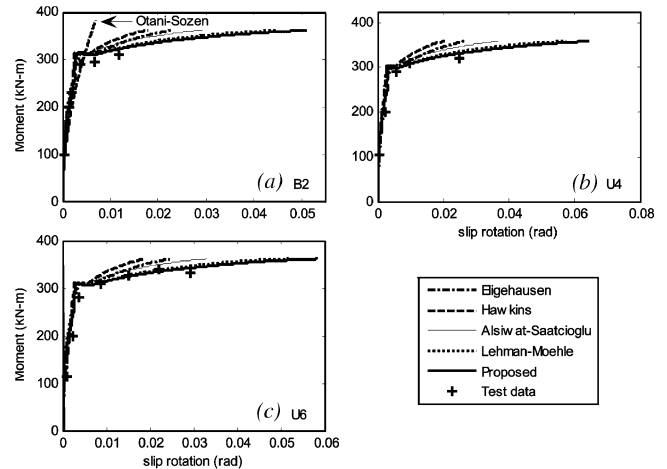


Fig. 12—Slip rotation predictions for: (a) Column B2; (b) Column U4; and (c) Column U6. (Note: 1 kN-m = 0.738 kip-ft.)

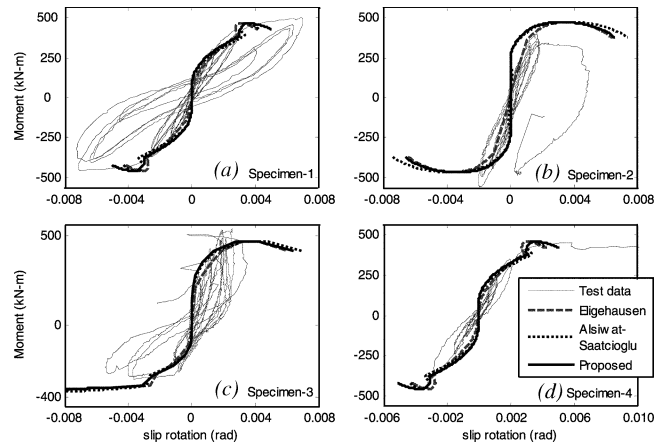


Fig. 13—Slip rotation predictions at base of: (a) Specimen 1; (b) Specimen 2; (c) Specimen 3; and (d) Specimen 4. (Note: 1 kN-m = 0.738 kip-ft.)

Table 2—Properties of test columns

Name	Reference	Column type*	Axial load, kN (kip)	Column height, mm (in.)	Cross section dimension,† mm (in.)	d_b , mm (in.)	f_y , MPa (ksi)	f'_c , MPa (ksi)
B2	10	C	600 (135)	900 (35.4)	350 (13.8)	25.4 (1.00)	438 (63.5)	40 (5.80)
U4	10	C	600 (135)	900 (35.4)	350 (13.8)	25.4 (1.00)	438 (63.5)	32 (4.64)
U6	10	C	600 (135)	900 (35.4)	350 (13.8)	25.4 (1.00)	438 (63.5)	37 (5.37)
Specimen 1	1	D	667 (150)	2946 (116.0)	457 (18.0)	28.7 (1.128)	434 (63.0)	21.2 (3.08)
Specimen 2	1	D	2670 (600)	2946 (116.0)	457 (18.0)	28.7 (1.128)	434 (63.0)	21.2 (3.08)
Specimen 3	1	D	‡	2946 (116.0)	457 (18.0)	28.7 (1.128)	434 (63.0)	21.2 (3.08)
Specimen 4	1	D	2670 (600)	2946 (116.0)	457 (18.0)	28.7 (1.128)	434 (63.0)	21.2 (3.08)

*C = cantilever; and D = double curvature.

†All specimens have square cross sections.

‡Varied from -267 to 2670 kN (-60 to 600 kip).

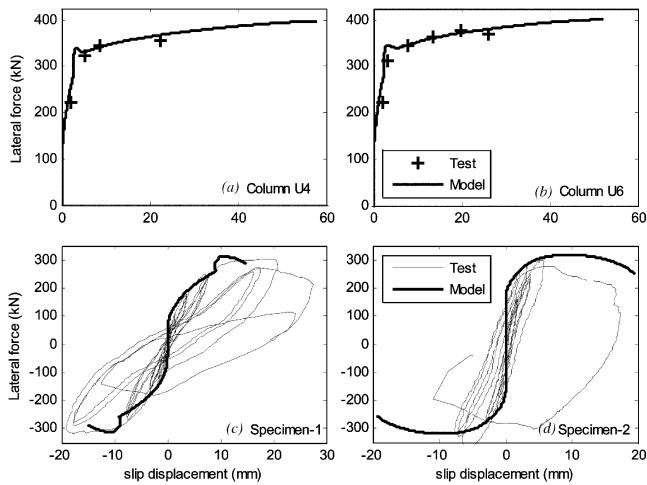


Fig. 14—Lateral load-slip displacement predictions using proposed model for: (a) Column U4; (b) Column U6; (c) Specimen 1; and (d) Specimen 2. (Note: 25.4 mm = 1 in.; 1 kN = 0.225 kip.)

Using Eq. (7) to calculate slip rotation causes some problems with the slip rotation predictions in the yield plateau region. Figures 12 and 13 show that all the models that use this equation for rotation calculations have a hook where the rotation decreases with increasing moment for a short period before continuing to increase again. When the tension steel yields in a concrete section, the neutral axis accelerates its migration towards the compression side of the section. This causes the denominator of Eq. (7) to increase rapidly, and the resulting slip rotation decreases. In the Alsiwat-Saatcioglu⁴ and proposed models, this problem is exacerbated by the small increase in slip calculated as the bar traverses the yield plateau. The proposed model predicts the slip rotation well overall, and this seems to outweigh the local problem in the yield plateau region predicted by the model.

Lateral displacement due to slip

Moment is induced into building columns through deformations and/or lateral loads applied at the column ends. The moment at the column ends is the product of the applied lateral load and the column height for a cantilever column, or half the height for a column with fixed ends. The lateral displacement due to slip Δ_s is calculated as

$$\Delta_s = \theta_s L \quad (20)$$

where θ_s is the slip rotation at the column end and L is the column height. Using these relationships, the lateral force-slip displacement diagram can easily be created from the moment-slip rotation relationship.

Slip rotations for the seven columns shown in Table 2 were obtained similarly by subtracting the flexural rotations from the measured total rotations at column end supports. The total end rotations are calculated as the difference between measurements of the vertical displacement transducers (within the 102 mm [4 in.] of the column ends) divided by the horizontal distance between the displacement transducers. To approximately separate the flexure and slip rotations, the average rotations along the column length were extrapolated

linearly to estimate actual rotation at the column ends. The remaining rotation was assigned to slip rotation.^{1,2}

Lateral force-slip displacement relationships calculated using the proposed model for Columns U4 and U6 and Specimens 1 and 2 are compared with the experimental data in Fig. 14. Results are similar to the moment-rotation results discussed previously. Overall, the monotonic envelopes predicted by the model fit the experimental data well.

DISCUSSION AND CONCLUSIONS

Test results show that the contribution of bar slip deformations to total member lateral displacement can be significant.¹ In addition to flexural deformations, bar slip deformations should be considered in modeling and analysis of reinforced concrete members. A monotonic reinforcement slip model is proposed and compared with five other analytical models.

It can be concluded that of the six models considered, five produce similar results (Fig. 10 and 12). These are the Hawkins,⁷ Eligehausen,⁶ Alsiwat-Saatcioglu,⁴ and Lehman-Moehle⁵ models and the proposed model. The first two of this list are numerical models that model the bond phenomenon on a detailed level. While the results obtained using the models presented by Hawkins⁷ and Eligehausen⁶ are better than the other models considered in some cases, implementation of these models in a structure-level analysis would be prohibitively expensive from a computational standpoint given the current state of computing technology. The three macro-level models examined all require a similar level of computational effort. The proposed model compares favorably with both the Lehman-Moehle⁵ and Alsiwat-Saatcioglu⁴ models based on the test data examined in this study (Fig. 12). The proposed model is used to calculate lateral load-slip displacement relations for seven columns from two different studies, and the computed relations compare well with the measured test results (Fig. 10 and 12 through 14).

ACKNOWLEDGMENTS

A part of this paper is based on work completed by the second author for his MS thesis. This work was completed under the support of a National Science Foundation Graduate Research Fellowship. The authors would like to thank J. P. Moehle of the University of California-Berkeley for reviewing this manuscript and for his feedback and thoughtful comments.

REFERENCES

1. Sezen, H., "Seismic Behavior and Modeling of Reinforced Concrete Building Columns," PhD thesis, University of California-Berkeley, Berkeley, CA, 2002, 324 pp.
2. Sezen, H., and Moehle, J. P., "Seismic Tests of Concrete Columns with Light Transverse Reinforcement," *ACI Structural Journal*, V. 103, No. 6, Nov.-Dec. 2006, pp. 842-849.
3. Otani, S., and Sozen, M. A., "Behavior of Multistory Reinforced Concrete Frames during Earthquakes," *Structural Research Series* No. 392, University of Illinois, Urbana, IL, 1972, 551 pp.
4. Alsiwat, J. M., and Saatcioglu, M., "Reinforcement Anchorage Slip Under Monotonic Loading," *Journal of Structural Engineering*, ASCE, V. 118, No. 9, Sept. 1992, pp. 2421-2438.
5. Lehman, D. E., and Moehle, J. P., "Seismic Performance of Well-Confined Concrete Bridge Columns," Report No. PEER-1998/01, University of California-Berkeley, Berkeley, CA, 2000, 316 pp.
6. Eligehausen, R.; Popov, E. P.; and Bertero, V. V., "Local Bond Stress-Slip Relationship of a Deformed Bar Under Generalized Excitations," Report No. UCB/EERC 83/23, University of California-Berkeley, Berkeley, CA, 1983, 169 pp.
7. Hawkins, N. M.; Lin, I. J.; and Jeang, F. L., "Local Bond Strength of Concrete for Cyclic Reversed Loadings," *Bond in Concrete*, Applied Science Publishers, London, UK, 1982, pp. 151-161.
8. Filippou, F. C.; Popov, E. P.; and Bertero, V. V., "Effects of Bond Deterioration on Hysteretic Behavior of Reinforced Concrete Joints," Report No. UCB/EERC 83/19, University of California-Berkeley, Berkeley, CA, 1983, 184 pp.

9. Soroushian, P., and Choi, K.-B., "Analytical Evaluation of Straight Bar Anchorage Design in Exterior Joints," *ACI Structural Journal*, V. 88, No. 2, Mar.-Apr. 1991, pp. 161-168.
10. Lowes, L. N.; Moehle, J. P.; and Govindjee, S., "A Concrete-Steel Bond Model for Use in Finite Element Modeling of Reinforced Concrete Structures," *ACI Structural Journal*, V. 101, No. 4, July-Aug. 2004, pp. 501-511.
11. Saatcioglu, M.; Alsiwat, J. M.; and Ozcebe, G., "Hysteretic Behavior of Anchorage Slip in R/C Members," *Journal of Structural Engineering*, ASCE, V. 118, No. 9, Sept. 1992, pp. 2439-2458.
12. ACI Committee 408, "Suggested Development, Splice, and Standard Hook Provisions for Deformed Bars in Tension (ACI 408.1R-79)," American Concrete Institute, Farmington Hills, MI, 1979, 3 pp.
13. Pochanart, S., and Harmon, T., "Bond-Slip Model for Generalized Excitation Including Fatigue," *ACI Materials Journal*, V. 86, No. 5, Sept.-Oct. 1989, pp. 465-474.
14. Ueda, T.; Lin, I. J.; and Hawkins, N. M., "Beam Bar Anchorage in Exterior Column-Beam Connections," *ACI JOURNAL, Proceedings* V. 83, No. 3, May-June 1986, pp. 412-422.
15. Lynn, A. C.; Moehle, J. P.; Mahin, S. A.; and Holmes, W. T., "Seismic Evaluation of Existing Reinforced Concrete Building Columns," *Earthquake Spectra*, EERI, V. 12, No. 4, Nov. 1996, pp. 715-739.
16. Sozen, M. A., and Moehle, J. P., "Development and Lap-Splice Lengths for Deformed Reinforcing Bars in Concrete," Report to the Portland Cement Association and Concrete Reinforcing Steel Institute, 1990.
17. Melek, M.; Wallace, J. W.; and Conte, J. P., "Experimental Assessment of Columns with Short Lap Splices Subjected to Cyclic Loads," *Report* No. PEER 2003/04, University of California-Berkeley, Berkeley, CA, 2003, 176 pp.
18. Setzler, E. J., "Modeling the Behavior of Lightly Reinforced Columns Subjected to Lateral Loads," MS thesis, Ohio State University, Columbus, OH, 2005, 202 pp.
19. ACI Committee 318, "Building Code Requirements for Structural Concrete (ACI 318-05) and Commentary (318R-05)," American Concrete Institute, Farmington Hills, MI, 2005, 430 pp.